



OPEN

Immunomodulatory effects of nanoparticles on dendritic cells in a model of allergic contact dermatitis: importance of PD-L2 expression

Angela Wong Lau¹, Jessica Perez Pineda¹ & Lisa A. DeLouise^{1,2}✉

Nanoparticle (NP) skin exposure is linked to an increased prevalence of allergic contact dermatitis. In our prior studies using the mouse contact hypersensitivity (CHS) model, we reported that silica 20 nm (SiO₂) NPs suppressed the allergic response and titanium dioxide NPs doped with manganese (mTiO₂) exacerbated it. In this work, we conducted *in vitro* experiments using bone marrow-derived dendritic cells (BMDCs) to study the combinatorial effect of the potent 2,4-dinitrofluorobenzene (DNFB) hapten sensitizer with SiO₂ and mTiO₂ NPs on BMDC cytotoxicity, cytokine secretion and phenotype using the B7 family ligands. Results show that DNFB and mTiO₂ behave similarly and exhibit proinflammatory characteristics while SiO₂ promotes a naive phenotype. We observe that the B7-H3 (CD276) ligand is only expressed on CD80+ (B7-1) BMDCs. Results from adoptive transfer CHS studies, combined with BMDC phenotype analysis, point to the importance of PD-L2 expression in modulating the adaptive immune response. This work identifies metrics that can be used to predict the effects of NPs on contact allergy and to guide efforts to engineer cell-based therapies to induce hapten specific immune tolerance.

The prevalence of allergic skin disorders and adverse skin reactions are on the rise worldwide, contributing to severe morbidity, and having a significant impact on the patient quality of life^{1,2}. It was estimated that the median prevalence of contact allergy is 21.2% (range 12.5–40.6%) in the general population of North America and Western Europe³. Irritant contact dermatitis results from an acute activation of the innate skin immune system following skin exposure to various types of chemicals (e.g. soaps, perfumes, solvents)⁴. Exposure to low molecular weight haptens can induce an adaptive immune response resulting in allergic contact dermatitis (ACD)^{4–7}. In the sensitization phase of ACD, antigen-presenting cells in the skin get activated. They uptake haptenized proteins and migrate to the skin-draining lymph nodes where they present antigen to naive T-cells that differentiate into CD8+ and/or CD4+ effector and memory T cells. Noncirculating tissue-resident memory (T_{rm}) cells seed the skin in 14–30 days and persist long term (> 1 year) in mouse models of ACD^{8,9}. In the challenge phase, re-exposure to the hapten activates the antigen-specific memory T cells to induce an allergic response.

There are numerous chemicals in the home, workplace, and in the environment that can contribute to irritant and/or ACD. Recent studies suggest that environmental factors, including nanoparticles (NPs), can influence the prevalence and course of allergic disease, and NPs are suspected to be a contributing factor to the rise of ACD^{10–12}. Sources of NPs are numerous. Natural sources include forest fires, soil erosion, dust storms, and volcanic activity, whereas anthropogenic sources include those produced in the laboratory for commercial use and those present in air pollution from factories, automobiles, and cigarette smoke^{13–15}. Particulates in air pollution are known to induce oxidative stress and inflammation in the skin^{16,17}. Studies suggest that oxidative stress in the skin is an initiating event that results in an immunosuppressive ACD response by activating the platelet-activating factor receptor (PAF-R) signaling pathway^{18,19}. Prior studies in our lab reported that engineered NPs can modulate the adaptive immune response in a mouse model of allergic contact hypersensitivity (CHS)²⁰. We observed that small (< 200 nm) negatively charged NPs, independent of composition, suppressed the allergic response in the

¹Department of Biomedical Engineering, University of Rochester, Rochester, NY, USA. ²Department of Dermatology, University of Rochester Medical Center, Rochester, NY, USA. ✉email: Lisa_DeLouise@urmc.rochester.edu

challenge phase but similar sized positive NPs did not²¹. Moreover, certain NPs including highly carboxylated carbon nanotubes (CNT) and some TiO₂ NPs could exacerbate the allergic response^{21–24}. The mechanisms of how NPs alter the adaptive immune response in the skin remain unclear, however, we did observe that NPs modulated early signaling events in the challenge phase (<2 h)²¹. Since, NPs do not readily diffuse through the skin barrier as small molecular weight chemical haptens^{20,25–29}, it seems plausible that the NPs must alter epidermal derived signals that can affect mast cell (MC) and/or dendritic cell (DC) activation or function. These two cell types are critically important in transducing the CHS allergic response^{30–32}. Mast cell deficiency in the skin dramatically reduces the allergic response due in part to impaired emigration of skin DCs to the lymph node in the sensitization phase^{32–34}. Activated MCs are an important source of TNF α that promotes DCs to migrate to lymph nodes³⁴. Furthermore, MCs and DCs interact to activate each other^{7,32}.

Recent studies in mice found that skin DCs (CD11c+, MHCII+), specifically epidermal Langerhans cells (CD103–, EpCAM+) and conventional cDC2 (CD103–, CD11c+, CD11b+), acquired OVA antigen in the skin and primed T cells in the lymph node but Langerhans cells were not required or sufficient to induce effector T cell response³⁵. In fact, the function of epidermal Langerhans cells in the development of the CHS adaptive immune response has been debated and intensely studied for years using genetic ablation strategies^{36–40}. It is now accepted that the intensity of the CHS response correlates directly with the efficiency of T cell priming, and that LCs are important only at low hapten exposure³⁸. Dermal DCs subsets, specifically cDC2, are mainly responsible for the initiation and activation of the CHS response^{31,38,41}. While, it is recognized that the physicochemical properties of NPs can alter DC function⁴², how NPs may alter phenotypic changes in cDC2 to effect the efficiency of T cell priming in the context of skin allergy is unknown.

In this work, we focus on examining the effect that NPs have on the phenotype and activation of bone marrow-derived (CD11c+, MHCII+) dendritic cells (BMDC). Specifically, we studied ~20 nm negatively charged silica (SiO₂) NPs that suppressed the in vivo CHS response and <100 nm negatively charged manganese-doped titanium dioxide NPs (mTiO₂) that exacerbated it²¹. Using flow cytometry, cytokine analysis, and the well-established dinitrofluorobenzene (DNFB) CHS mouse model, we characterized the BMDC phenotype focusing on several B7 family of co-stimulatory markers⁴³ including CD80 (B7-1), CD86 (B7-2), PD-L1 (B7-H1), PD-L2 (B7-DC) and CD276 (B7-H3). The rationale for selecting these markers is given below.

CD86 and CD80 are classic markers of DC activation and they have dual binding capacity to CD28, an activating T cell receptor that is constitutively expressed on naïve T cells and CTLA-4 a regulatory receptor which is upregulated upon T cell activation⁴⁴. The dual binding capacity of CD86/CD80 to T cell receptors that enhance (CD28) or suppress (CTLA-4) proliferation has been the subject of much investigation^{45–48}. CD80 and CD86 act cooperatively to modulate T-cell activation and tolerance induction^{43,47}. It is believed that T cell fate is driven by the relative expression levels of the CD86/CD80 ligands on the DC and the CD28/CTLA-4 T cell receptors^{46,49,50} as well as the fact that the binding affinity of CD86 and CD80 ligands to CTLA-4 is ~10× stronger than to CD28 which leads to competitive binding between the activating and regulatory receptors^{44,51,52}.

Programmed death ligand 1 (PD-L1) and PD-L2 are ligands expressed on DCs that bind the PD-1 receptor on activated T-cells. Activation of the PD1 receptor inhibits T cell proliferation and proinflammatory cytokine production to suppress immune responses⁵³. PD-L1 (B7-H1) is widely expressed on many cell types, including cancer cells, whereas PD-L2 (B7-DC) is only expressed on DCs⁵². It is reported that PD-L2 binds PD-1 with two to sixfold stronger affinity compared with PD-L1^{54,55}. Others report that PD-L1 and PD-L2 bind PD-1 with comparable affinities but exhibit striking differences in their PD1 receptor association and dissociation characteristics⁵⁶. Since PD-L1 and PD-L2 expression levels depend on distinct stimuli, it is suggested that they may have overlapping and differential roles in regulating T_H1 and T_H2 T cell responses^{56,57}. Studies suggest PD-L2 positive DCs are needed to induce allergen tolerance by generating regulatory T cells (T regs)⁵⁸ and they contribute to generating potent LAP + Tregs³⁵.

CD276 (B7-H3) is a member of the B7 immune checkpoint family and is thought to promote an immunosuppressive response as it is highly expressed in many cancers that correlate with poor clinical outcomes⁵⁹. Our interest in this marker stems from a study that showed activation of the arylhydrocarbon receptor in BMDCs generated Tregs cells that suppressed the allergic CHS response in mice⁶⁰. Analysis of the DC markers (MHCII, CD86, PD-L1, B7-H3, B7-H4) following arylhydrocarbon receptor agonist exposure revealed a marked upregulation of B7-H3 which was associated with the immunosuppression⁶⁰.

In this study we identified key markers of BMDC activation by proinflammatory stimuli (lipopolysaccharide, DNFB, mTiO₂) including a upregulation of the CD86, CD80, and PD-L1 (B7-H1), as well as an upregulation of CD276 (B7-H3) and a negligible to slight downregulation of PD-L2 (B7-DC). Because of the dual binding affinity of CD80 and CD86 ligands to the CTL-4 (regulatory) and CD28 (activating) T-cell receptors, we further examined how the expression levels of PD-L1, PD-L2 and CD276 differed among the CD80/CD86 subpopulations compared to unstimulated immature BMDCs (imDCs). We observe that CD276 is only expressed on CD80+ cells and that both NPs modulate its expression. In single exposure studies, we find that DNFB and mTiO₂ behave similarly and exhibit proinflammatory characteristics. In contrast, SiO₂ is cytoprotective and promotes a naïve imDC phenotype, particularly in DNFB co-culture studies. While PD-L1 is upregulated by proinflammatory stressors, PD-L2 is not and in fact, is down regulated by mTiO₂ exposure which correlates with an exacerbation of the allergic response in the in vivo adoptive transfer contact hypersensitivity (CHS) mouse model. These results show that NPs co-cultured with a potent sensitizer can alter the BMDC phenotype to effect the efficiency of T cell priming and the intensity of the CHS response in both the sensitization and challenge phases. This work points to metrics that can be used to predict the effects of NPs on contact allergy and to the novel use of NPs to engineer immunomodulatory responses in contact allergy.

Results

Effects of DNFB, SiO₂ and mTiO₂ on BMDC toxicity, cytokine secretion and co-stimulatory molecule expression

We performed cytotoxicity studies to establish concentration ranges to examine the effects of NPs and DNFB on BMDC phenotypes. We conducted single exposure studies to each stressor for 1 h to measure cytotoxicity as a function of concentration using the flow cytometry. Results (Fig. 1A) show a significant dose-dependent decrease in cell viability for DNFB and mTiO₂ but not for SiO₂. Exposing cells for 1 h to DNFB (0.1 mM) or mTiO₂ (0.05 mg/mL) caused a ~50% decrease in cell viability whereas exposing cells to SiO₂ was not cytotoxic. The effects of DNFB exposure correlated with notable changes in the BMDC morphology viewed in bright-field and in TEM images, with cells becoming round and losing dendrites (Figs. S1–S2). NP uptake in endosomal vesicles was also confirmed (Figs. S3–S4). Non-cytotoxic concentrations of each stressor were selected and the BMDCs were exposed for 5 h, 15 h, and 24 h (Fig. 1B). Results again show a significant decrease in cell viability over time for DNFB (0.001 mM) and mTiO₂ (0.005 mg/mL) but not for SiO₂ (0.01 mg/mL). The dose and time dependent cytotoxicity flow cytometry results were consistent with results using the PrestoBlue assay (Fig. S5).

Cytotoxicity studies suggest that DNFB and mTiO₂ behave similarly and are likely potent proinflammatory stressors compared to SiO₂. To further characterize interactions with BMDCs, we evaluated the key proinflammatory (IL-6, TNF α) and immunosuppressive (IL-10) cytokines secreted in the supernatant by ELISA. BMDCs were exposed to DNFB (0.001 mM), SiO₂ (0.01 mg/mL) and TiO₂ (0.005 mg/mL) as a function of time. Results showed that each compound increased IL-6 (Fig. 2A) and TNF α (Fig. 2B) secretion and exposure to mTiO₂ upregulated IL-10 (Fig. 2C). One-hour exposures as a function of concentration also showed that mTiO₂ upregulated IL-6,

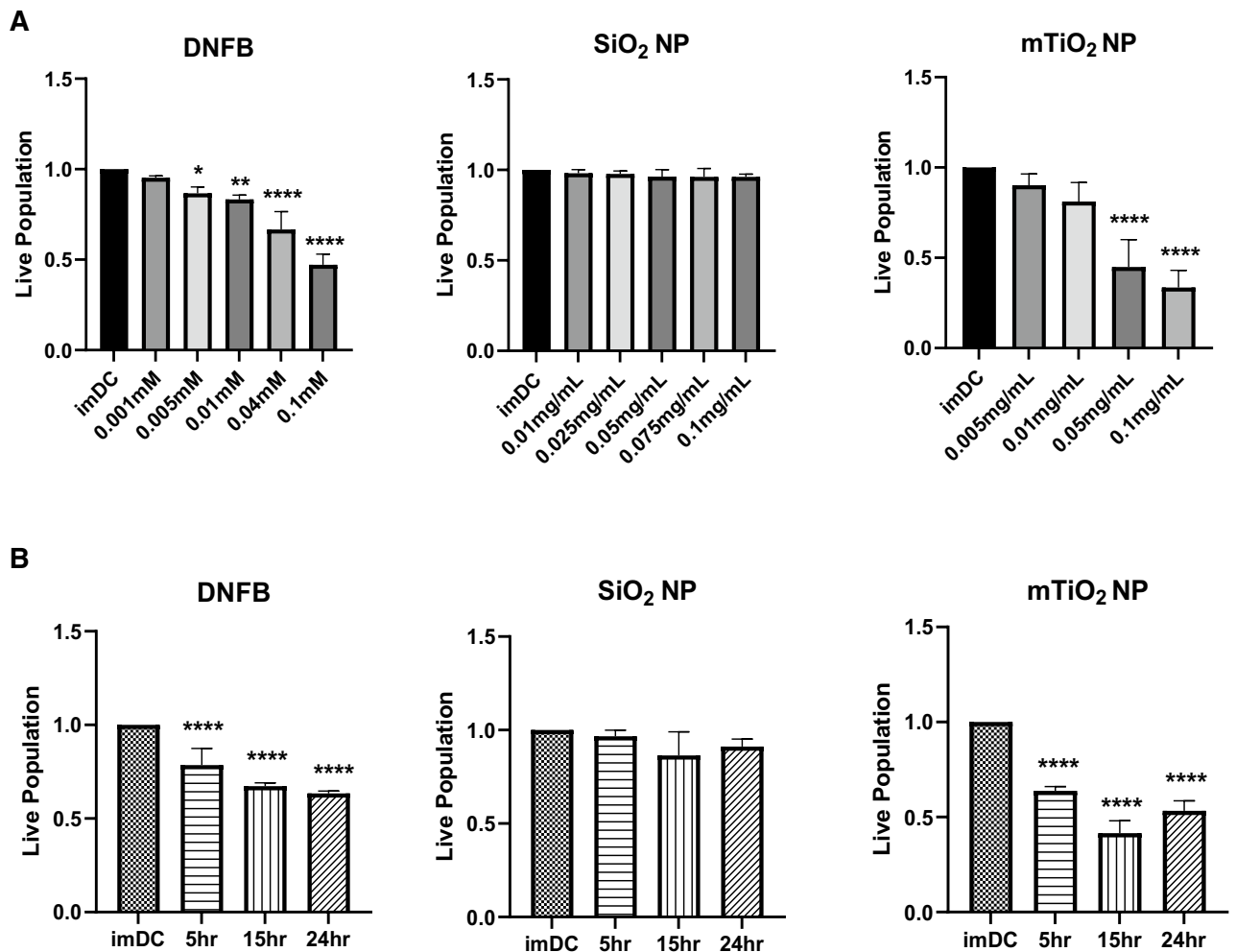


Figure 1. Effects of DNFB, SiO₂ and mTiO₂ exposure on BMDC cytotoxicity as a function of concentration and time. BMDCs were harvested on day 8 and treated with DNFB, SiO₂ and mTiO₂ to study cytotoxicity as a function of concentration and time by flow cytometry. (A) Cell viability as a function of concentration for a 1 h exposure. (B) Cell viability following exposure to the lowest non-cytotoxic concentrations from (A) and exposed over a period of 5 h, 15 h and 24 h. Results indicate that cytotoxicity of DNFB and mTiO₂ NPs on BMDCs was dose- and time- dependent. Live population was normalized the imDC no treatment control. Ordinary one-way ANOVA was performed and compared to imDC. N = 3–5. Mean \pm SD. * p < 0.05, ** p < 0.01, *** p < 0.001, **** p < 0.0001.

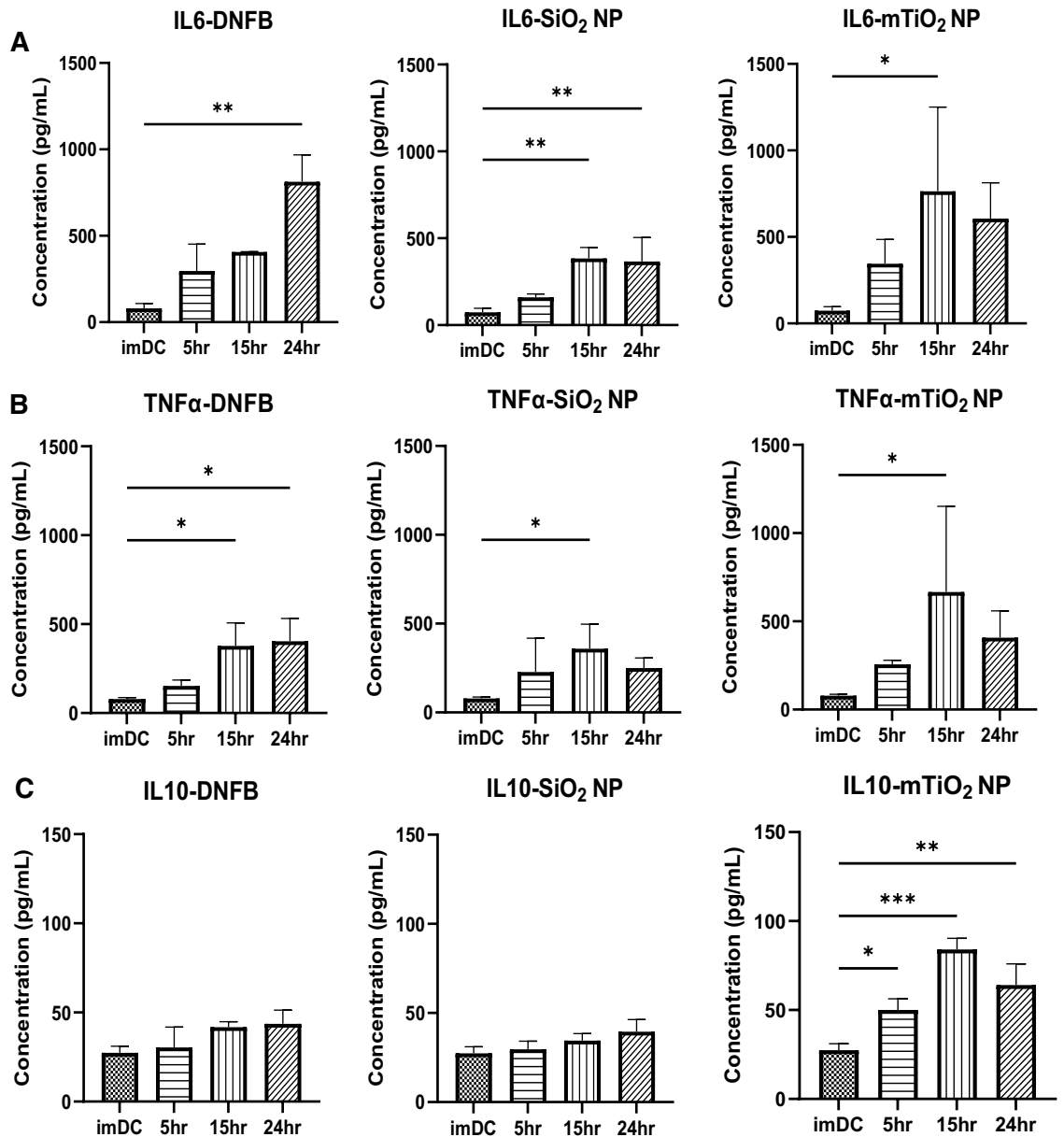


Figure 2. Effects of DNFB, SiO₂ and mTiO₂ exposure on BMDC cytokine secretion. BMDCs were exposed to a low non-cytotoxic concentrations of each stressor (0.001 mM DNFB, 0.01 mg/mL SiO₂ and 0.005 mg/mL mTiO₂) over a period of 5 h, 15 h and 24 h. ELISA was used to analyze cytokines in cell culture supernatants: (A) IL-6, (B) TNFα, (C) IL-10. All stressors tend to increase IL-6 and TNFα. Only mTiO₂ increased IL-10. Concentration was normalized against % of live cells. Ordinary one-way ANOVA was performed and compared to imDC. N = 3–5. Mean ± SD. *p < 0.05, **p < 0.01, ***p < 0.001, ****p < 0.0001.

TNFα, and IL-10 (Fig. S6). These results suggest that mTiO₂ is a potent proinflammatory stressor, behaving similarly to lipopolysaccharide (LPS) (50 ng/mL), that also upregulated IL-6, TNFα and IL-10 (Fig. S7). These observations were corroborated by intracellular flow cytometry staining for IL-10 and TNFα as a function of concentration and time (Figs. S8–S9) but in contrast to mTiO₂, we observe that SiO₂ tended to upregulate IL-10 without upregulating TNFα which, may suggest an immunosuppressive potential for SiO₂ exposure.

Next, we examined the effect of each stressor on the phenotype of the BMDCs by measuring the expression levels of the co-stimulatory molecules by flow cytometry. Single and double gating strategies, with FMO controls, were used (Fig. S10A–C). Single gating assesses the expression levels of each marker on the live cell population. Double gating analyzes the CD11c + MHCII+ subpopulation. To interpret results, we compared them to LPS exposure (50 ng/mL) over time which, for single gating (Fig. S11) and double gating (Fig. S12), induced the expression of CD86, CD80, and PD-L1. CD276 increased early (3–6 h) and then returned to baseline and no changes in PD-L2 expression were induced by LPS. For single gating, exposing BMDCs to DNFB (0.001 mM), SiO₂ (0.01 mg/mL), and mTiO₂ (0.005 mg/mL) caused differential changes in the CD11c + MHCII+ phenotype as a function of time (Fig. 3) with DNFB producing effects most similar to LPS exposure. DNFB and mTiO₂

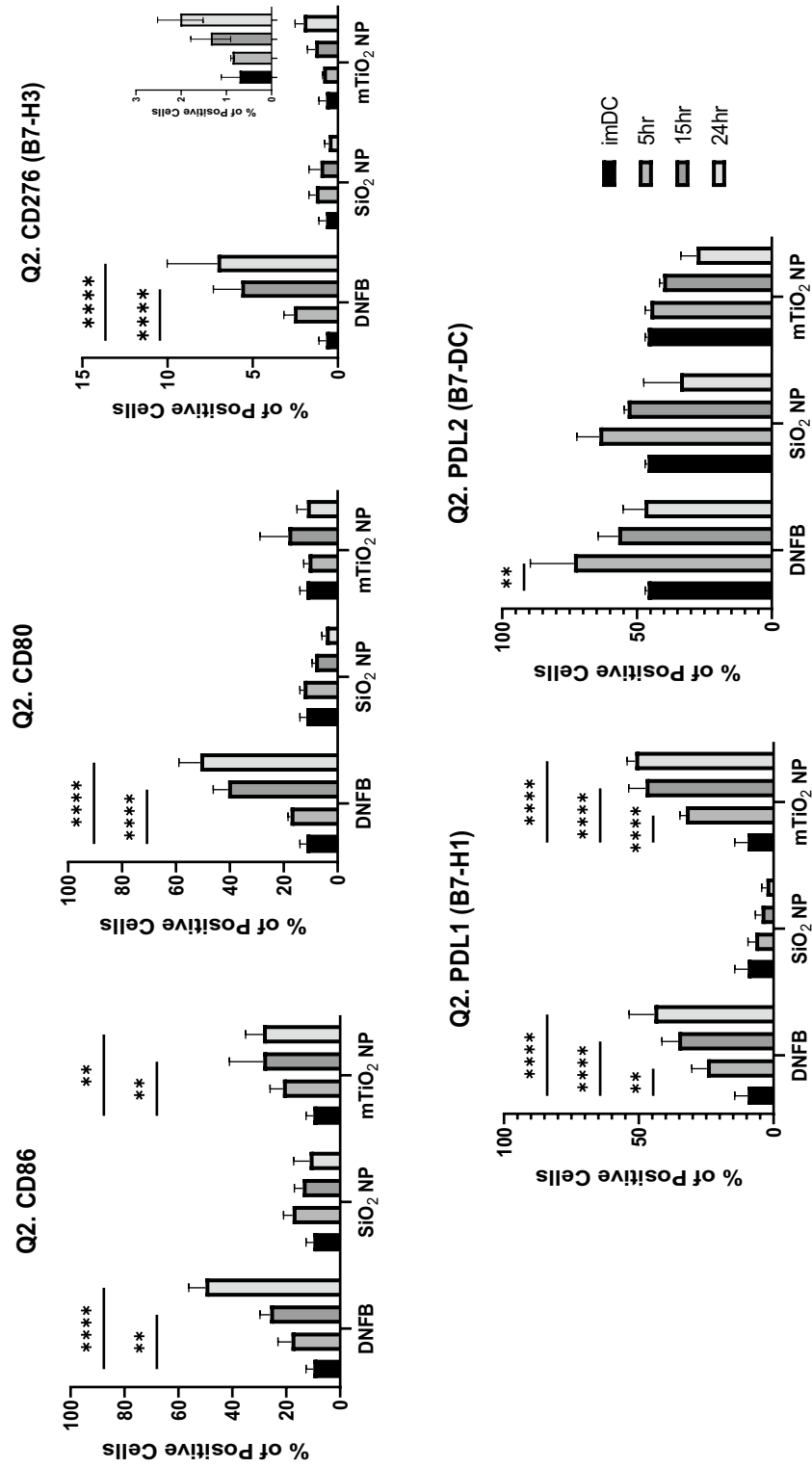


Figure 3. Co-stimulatory molecules from the B7 family quantified by flow cytometry gated on the CD11c+ MHCII + subpopulation following BMDC exposure to each stressor over time. The phenotypic characteristics of BMDCs following exposure to a low concentration of each stressor (0.001 mM DNFB, 0.01 mg/mL SiO₂ and 0.005 mg/mL mTiO₂) was followed over time by flow cytometry gated under the CD11c+ MHCII + (Q2.) subpopulation. DNFB and mTiO₂ behave more similar with upregulation of CD86, CD276, and PD-L1 over time. Only DNFB upregulated CD80. Exposure to SiO₂ did not alter these B7 ligands over time. Ordinary one-way ANOVA was performed and compared to imDC. N = 3–5. Mean ± SD. *p < 0.05, **p < 0.01, ***p < 0.001, ****p < 0.0001.

upregulated CD86 and PD-L1 expression whereas CD80 and CD276 were only upregulated by DNFB over time. PD-L2 was expressed on ~50% of imDC and exposure to each stressor did not alter its expression. Exposure to SiO₂ did not alter any co-stimulatory molecule suggesting BMDC maintained a naïve phenotype. Taken together, the results suggest that DNFB and mTiO₂ induce an activated BMDC phenotype and that mTiO₂ may be a more potent stressor as it failed to upregulate CD80, which is important for binding CTLA-4 to promote regulation.

The differential effects of each stressor on the expression of CD80 and CD86 led us to investigating the expression of PD-L1, PD-L2, and CD276 within the CD86/CD80 subpopulations over time (Fig. 4). Results showed that exposure to DNFB (0.001 mM) decreased the naïve CD80-CD86- double negative (DN) population and induced a steady significant rise in the activated CD80⁺CD86⁺ double positive (DP) population which are trends expected for a proinflammatory stressor. Similarly, mTiO₂ (0.005 mg/mL) showed a trend toward upregulating the DP population, whereas SiO₂ (0.01 mg/mL) exposure over time did not. Both NPs tended to downregulate slightly the DN subpopulation up to 15 h but not as definitively as DNFB. This subtle decrease in the DN is due primarily to the upregulation of CD80⁺ single-positive cells (Fig. S13). The expression levels of CD276, PD-L1 and PD-L2 in the CD80/CD86 subpopulations also differed depending on the stressor, with DNFB and mTiO₂ exhibiting similar trends. Specifically, DNFB and mTiO₂ exposure up-regulated PD-L1 in the DN (Fig. 4) and the single positive subpopulations (Fig. S13) with no change in the DP subpopulations. In contrast, SiO₂ exposure down-regulated PD-L1 expression in the DP subpopulation over time with no change in DN subpopulation. No changes in PD-L2 expression in DP or DN subpopulations were induced by either stressor (Fig. 4) but decreases in PD-L2 expression in the CD86 and CD80 single positive cells were induced by SiO₂ only (Fig. S13). CD276 was only expressed CD80⁺ single (Fig. S13) and double positive cells (Fig. 4). Both NPs tended to increase CD276 on the activated DP cells at 24 h. In summary, this data shows that DNFB and mTiO₂ exposure promotes the upregulation of the activated DP phenotype, and increased PD-L1 expression in the naïve DN population over time. PD-L1 expression of an activated DP population was unchanged over time with exposure to DNFB and mTiO₂, whereas SiO₂ exposure tended to decrease PD-L1 expression pointing again to the similarities between DNFB and mTiO₂.

Effects of DNFB co-exposure with NPs on cytotoxicity, cytokine secretion and co-stimulatory molecule expression

In prior studies, NPs co-exposed with DNFB modulated the *in vivo* CHS response in the challenge phase²¹. In this work, we were able to observe clear differences between SiO₂ and mTiO₂ in single exposure studies of cytotoxicity, cytokine production, and on phenotypic alterations of BMDC, with mTiO₂ behaving more similarly to DNFB. Here, we studied the effects of DNFB co-exposure with NPs on cytotoxicity and cytokine secretion compared to DNFB alone at 1 h (Fig. S14 and 24 h (Fig. 5). Consistent with earlier studies (Fig. 1), BMDC cultured with DNFB (0.001 mM) alone for 24 h was cytotoxic. Co-culture with SiO₂ (0.01 mg/mL) showed a protective effect (Fig. 5A). In contrast, co-culture with mTiO₂ (0.005 mg/mL) significantly exacerbated the toxic response (Fig. 5B). A cytoprotective effect of SiO₂ was also observed at 1 h exposure (Fig. S14) and is consistent with prior studies in keratinocytes²³ and fibroblasts⁶¹. We also tested the supernatant of each treatment group for IL-6, TNF α , and IL-10 by ELISA. Results show a downregulation of IL-6 with DNFB co-cultured with SiO₂ but not with mTiO₂ (Fig. 5C,D). Co-culture with either NP did not alter the levels of TNF α produced by DNFB exposure at 24 h (Fig. 5E,F) however, co-culture for 1 h with mTiO₂, but not SiO₂ NPs, showed elevated IL-6 levels (Fig. S14D) and both NPs elevated TNF α above that produced by DNFB at 1 h (Fig. S14E,F). Co-culture with mTiO₂, but not SiO₂ at 24 h (Fig. 5G,H), increased the secretion of IL-10, which is consistent with the mTiO₂ single exposure studies (Fig. 2). These co-culture studies demonstrate that SiO₂ exhibits a cytoprotective against effect DNFB exposure and exhibits an immunosuppressive effect as measured by a reduction in IL-6 secretion.

Next, the effects of DNFB co-exposure with NPs on the expression of the costimulatory molecules was investigated using flow cytometry (Fig. 6). Double gating on the CD11c⁺MHCII⁺ subpopulation showed that co-exposing BMDC to DNFB (0.001 mM) with either SiO₂ (0.01 mg/mL) or mTiO₂ (0.005 mg/mL) similarly down-regulated the DNFB activation of CD86, CD80, CD276, and PD-L1. Co-exposure with mTiO₂ tended to downregulate PD-L2 expression to levels below the imDC levels.

Differentiating the effects of DNFB co-exposure with NPs on the expression levels of PD-L1, PD-L2 and CD276 in the BMDC CD80/CD86 subpopulations was less clear (Fig. 7). Consistent with single exposure studies at 24 h (Fig. 4), DNFB activates the BMDCs as evidenced by an increase in the C86⁺CD80⁺ DP subpopulation and a decrease the naïve C86⁻CD80⁻ DN subpopulation. Both NPs suppressed BMDC activation, maintaining the DP and DN subpopulations to imDC levels at 24 h. There were no statistically significant changes in CD276 expression. However, both NPs co-cultured with DNFB increased PD-L1 expression on the DP subpopulation at 24 h, which was also evident at 1 h for mTiO₂, but not for SiO₂, which exhibited a statistically significant decrease PD-L1 at 1 h relative to the imDC (Fig. S15). The most intriguing differential effect between the NPs co-cultured with DNFB was the observation that mTiO₂ induced a significant decrease in PD-L2 expression in the DP subpopulation at 24 h and SiO₂ did not (Fig. 7). This decrease was also evident after only 1 h of co-culture (Fig. S15). A second, potentially important difference between the NPs was observed at 1 h exposure in PD-L1 expression on the DP subpopulation where SiO₂ decreased expression whereas mTiO₂ upregulated it over DNFB levels (Fig. S15). However, at 24 h both NPs increased PD-L1 on the activated DP cells and decreased PD-L2 expression on the naïve DN cells. Statistically significant changes in PD-L2 expression were not observed in the activated DP or the naïve DN subpopulations in single-exposure studies (Fig. 4). The significant differences in PD-L1 and PD-L2 expression in the activated DP subpopulation caused by mTiO₂ co-cultured with DNFB and the opposing effects with SiO₂ co-culture maybe influential in the BMDC controlling the fate of the adaptive immune response.

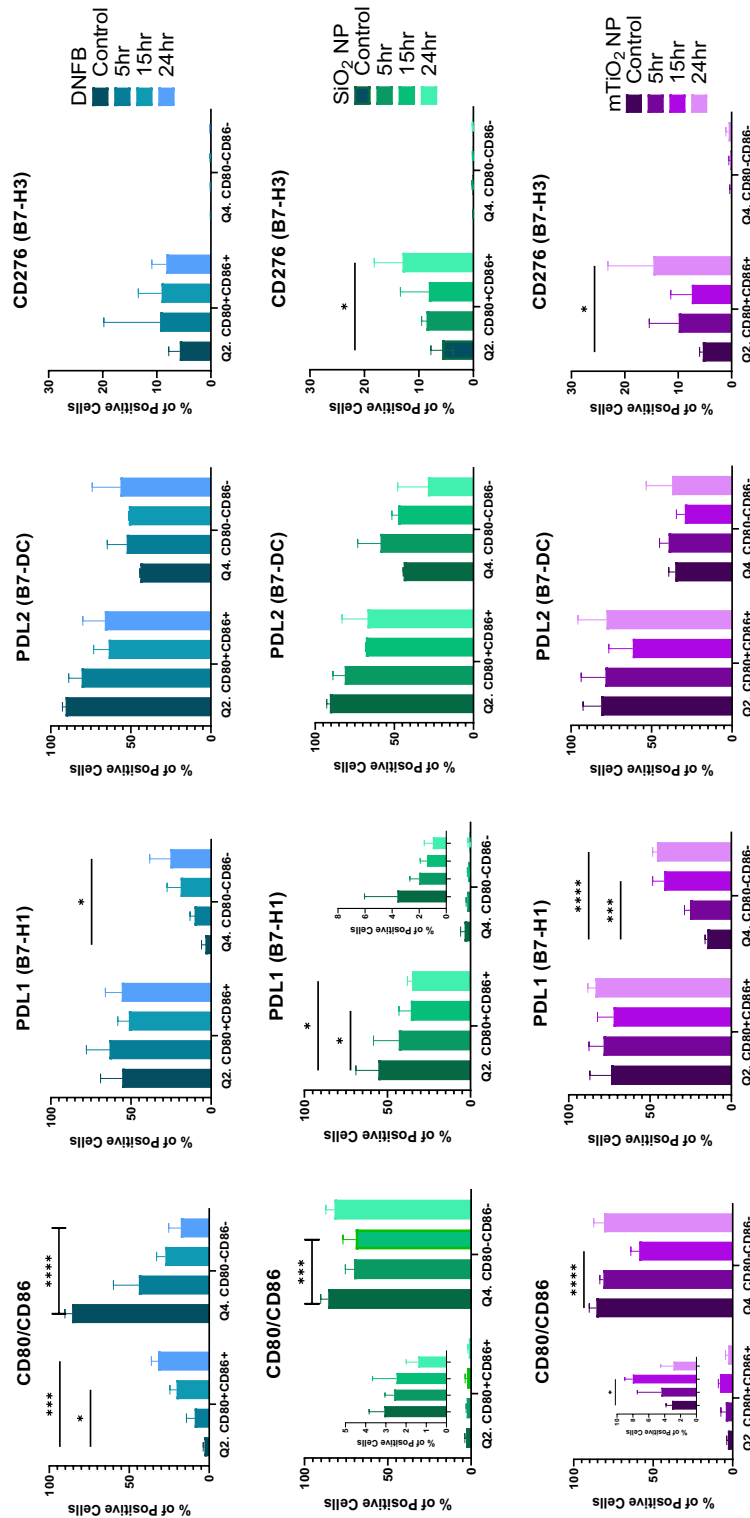


Figure 4. Co-stimulatory molecules from the B7 family quantified by flow cytometry gated on the CD11c+ MHCII+ and CD80/CD86 subpopulations following BMDC exposure to each stressor over time. Results for DNFB are colored in blue, SiO₂ in green and mTiO₂ in purple. The phenotypic characteristics of BMDCs following exposure to a low concentration of each stressor (0.001 mM DNFB, 0.01 mg/mL SiO₂ and 0.005 mg/mL mTiO₂) was followed over time, 5 h, 15 h, and 24 h, by flow cytometry gated under the CD11c+ MHCII+ CD80/CD86 subpopulations. Presented here are changes the CD80+ CD86+ double positive (DP) (Q2.) and the CD80- CD86- double negative (DN) (Q4.) subpopulations including the expression levels of PD-L1 (B7-H1), PD-L2 (B7-DC) and CD276 (B7-H3) on the DP and DN subpopulations. For DNFB exposure, the activated DP population clearly increases as the naive DN decreases and PD-L1 expression increased on the DN at 24 h. mTiO₂ exposure over time parallels the effects of DNFB exposure. In contrast, SiO₂ exposure over time tended to decrease the DP subpopulation and it significantly decreased PD-L1 expression in the DP subpopulation. Both SiO₂ and mTiO₂ tended to increase CD276 in the DP at 24 h. The similarities between DNFB and mTiO₂ were evident in CD80/CD86 and PD-L1 expression and distinct from SiO₂. A two-way ANOVA was performed and compared to imDC. N = 3–5. Mean ± SD. *p < 0.05, **p < 0.01, ***p < 0.001, ****p < 0.0001.

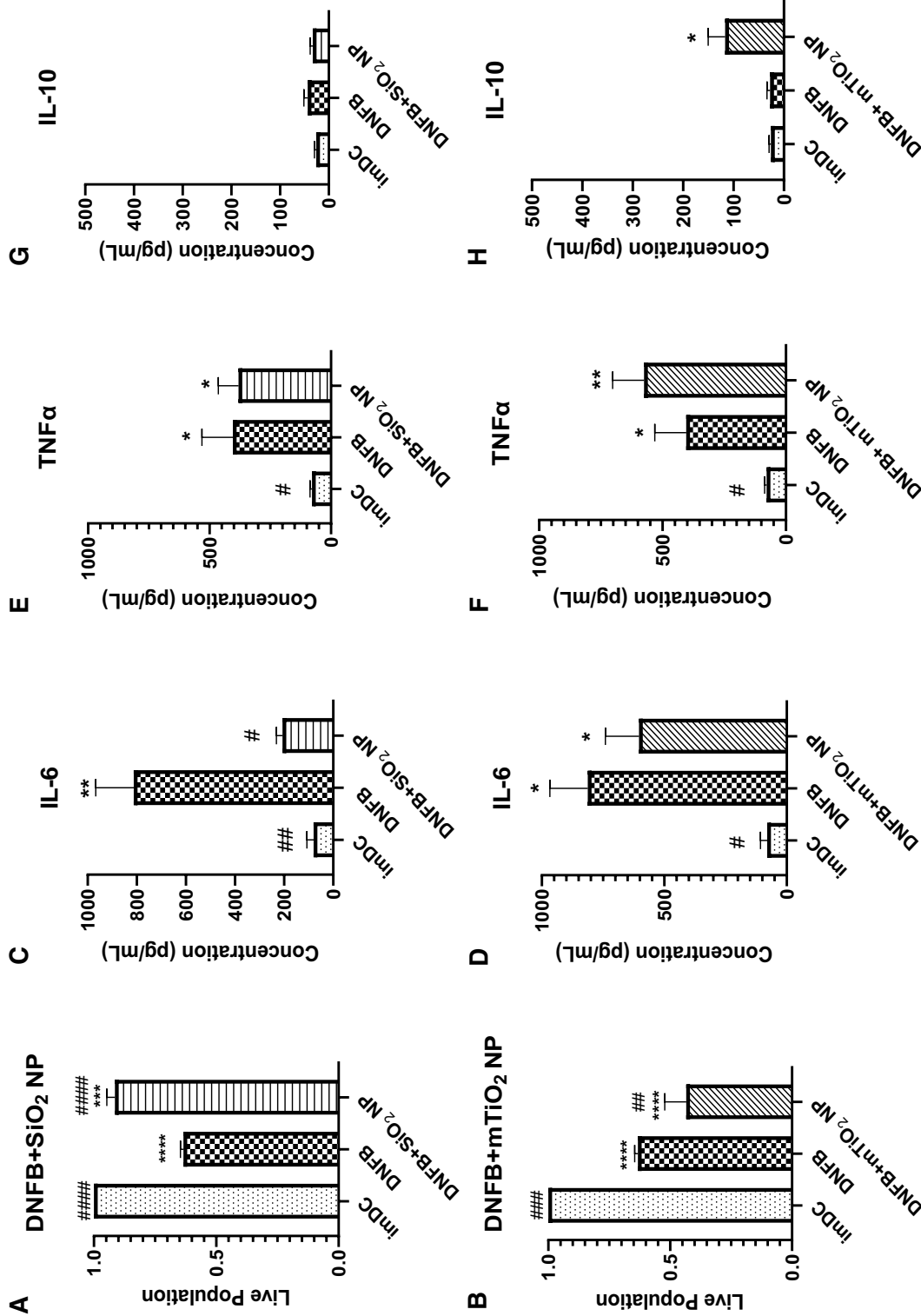


Figure 5. BMDC cytotoxicity and cytokine secretion following co-exposure to DNFB with SiO₂ or mTiO₂ NPs. BMDCs were co-exposed to DNFB plus SiO₂ or mTiO₂ nanoparticles for 24 h. Cell viability and secreted cytokines were measured and compared to DNFB treatment alone and to untreated imDC as a control. (A) SiO₂ NPs were shown to have cytoprotective effect in DNFB co-exposure whereas (B) mTiO₂ NPs induced higher cytotoxicity. Supernatants were collected to analyze cytokine production by ELISA for (C,D) IL-6 which showed co-culture with SiO₂ NPs decreased IL-6 production while co-culture with mTiO₂ did not. (E,F) addition of either NPs did not alter the levels of TNFα produced by DNFB alone and (G,H) the co-culture of DNFB with mTiO₂ NPs increased IL-10 production while SiO₂ NPs did not. Ordinary one-way ANOVA was performed and compared to imDC (*), and DNFB alone (#). Concentration was normalized against % of live cells. N = 3–5. Mean ± SD. *[#]p < 0.05, **[#]p < 0.01, ***[#]p < 0.001, ****[#]p < 0.0001.

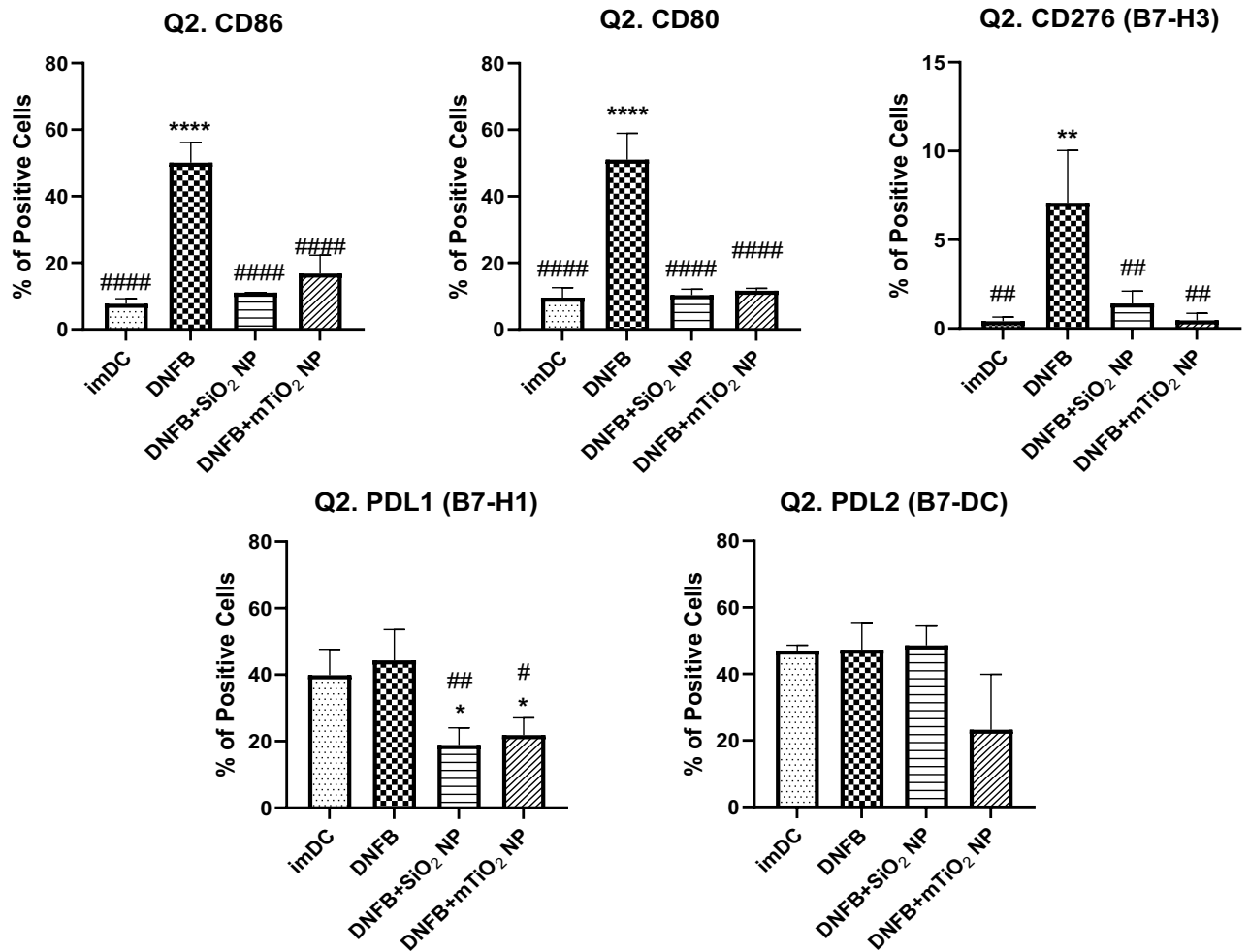


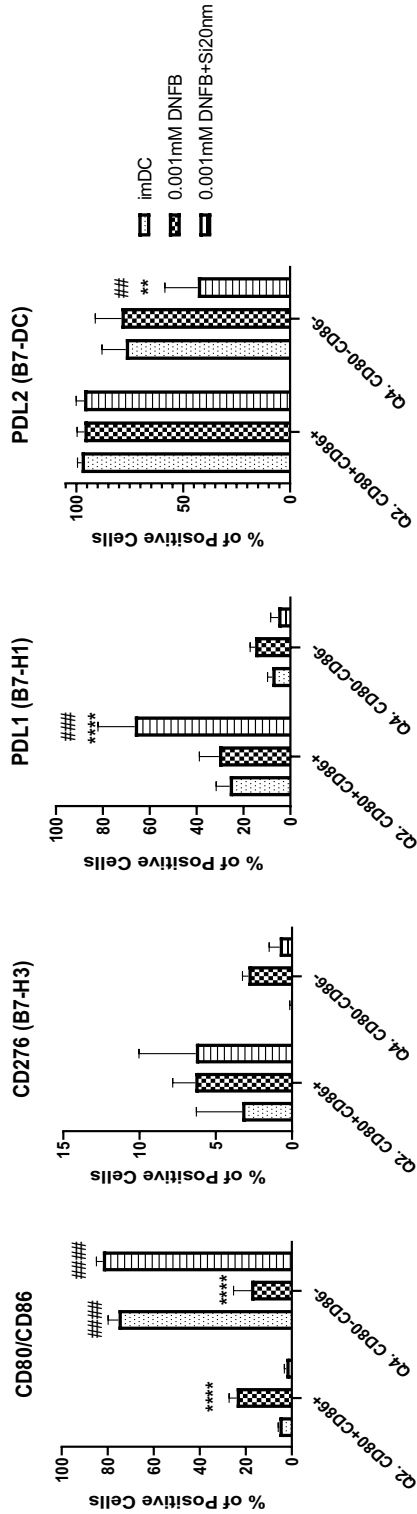
Figure 6. Co-stimulatory molecules from the B7 family quantified by flow cytometry gated on the CD11c + MHCII + subpopulation following co-exposure of DNFB with NPs. BMDCs were treated with DNFB (0.001 mM DNFB) and co-exposed with SiO₂ (0.01 mg/mL) or mTiO₂ (0.005 mg/mL) NPs for 24 h. Surprisingly, both NPs appeared to suppress the activation of all co-stimulatory molecules relative to DNFB only at 24 h, except for PD-L2, for which mTiO₂ significantly down regulated it. Ordinary one-way ANOVA was performed and compared to imDC (*) and DNFB (#). N = 3–5. Mean ± SD. */# p < 0.05, **/# p < 0.01, ***/### p < 0.001, ****/#### p < 0.0001.

Effects of NPs on the sensitization and challenge phases using the in vivo DNFB contact hypersensitivity model

Analysis of cytotoxicity, cytokine secretion and co-stimulatory markers taken together suggest that DNFB + SiO₂ co-exposure tends to promote a more naïve or regulatory BMDC phenotype, whereas DNFB + mTiO₂ promoted a proinflammatory BMDC phenotype. To test this, we used the in vivo CHS mouse model with adoptive transfer. We first tested the difference between topical and subcutaneous (S.C.) DNFB sensitization. BMDCs were treated with DNFB (0.01 mM) for 1 h. After two wash steps, the cells were resuspended in sterile saline and injected S.C. to sensitize the mice. A second group of mice was topically sensitized by applying 20 µL of 0.05% DNFB in acetone:olive oil vehicle (4:1)^{7,21,60}. Five days later, ear thickness was measured, and the mice were challenged with 0.2% DNFB on one ear and with vehicle on the other. On day 6, ear thicknesses were remeasured. Results of ear swelling response showed no difference between the topical sensitization and S.C. sensitization (Fig. 8A).

In prior work we observed an immunomodulatory effect of NPs in the challenge phase with DNFB topical sensitization²¹. To test if these effects are similarly observed with S.C. sensitization, we S.C. sensitized the mice with BMDC treated with 0.01 mM DNFB for 1 h. We challenged the mice on Day 5 with 0.2% DNFB alone, or mixed with NPs and measured the ear thickness on Day 6. Results show a similar result to our previous data²¹ indicating that SiO₂ NPs suppressed and mTiO₂ NPs exacerbated the allergic response relative to challenge with DNFB alone (Fig. 8B). Next, we compared S.C. sensitization using BMDC treated with DNFB (0.01 mM) alone or BMDC co-cultured with SiO₂ (0.01 mg/mL) or mTiO₂ (0.005 mg/mL) for 1 h. After two wash steps, we S.C. injected the cells to sensitize the mice. Upon challenge, we treated one ear with 0.2% DNFB and the other with vehicle. Results show that mice sensitized with BMDC treated with DNFB + SiO₂ measured a decreased ear swelling relative to DNFB alone. In contrast, mice S.C. sensitized with BMDC treated with DNFB + mTiO₂ showed an

A. SiO₂ NP



B. mTiO₂ NP

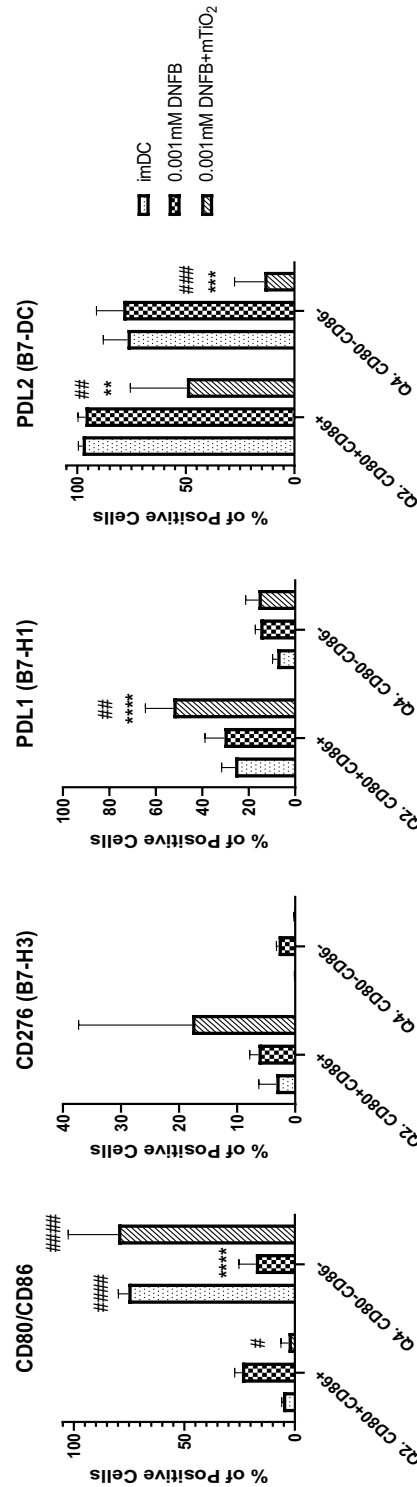


Figure 7. Co-stimulatory molecules from the B7 family quantified by flow cytometry gated on the CD11c+ MHCII + CD80/CD86 subpopulations following 24 h DNFB alone or DNFB plus NP co-exposure. CD80/CD86 subpopulations were divided and CD276 (B7-H3), PD-L1 (B7-H1) and PD-L2 (B7-DC) were gated under, double positive (DP) population (Q2.) or double negative (DN) population (Q4.) to determine whether their expression varies under the different activation states of BMDCs by using the activation markers CD80/CD86 following non-cytotoxic concentrations of (A) 0.001 mM DNFB alone and plus 0.01 mg/mL SiO₂ co-exposure and (B) 0.001 mM DNFB alone and plus 0.005 mg/mL mTiO₂ co-exposure. NPs suppressed BMDCs activation, increased PD-L1 expression and mTiO₂ induced a significant decrease in PD-L2 expression in the DP subpopulation at 24 h while SiO₂ did not. A two-way ANOVA was performed and compared to imDC (*), and DNFB (#). N = 3–5. Mean ± SD. **/##/###/****/##### p < 0.01, ***/###/####/##### p < 0.001, ****/####/##### p < 0.0001.

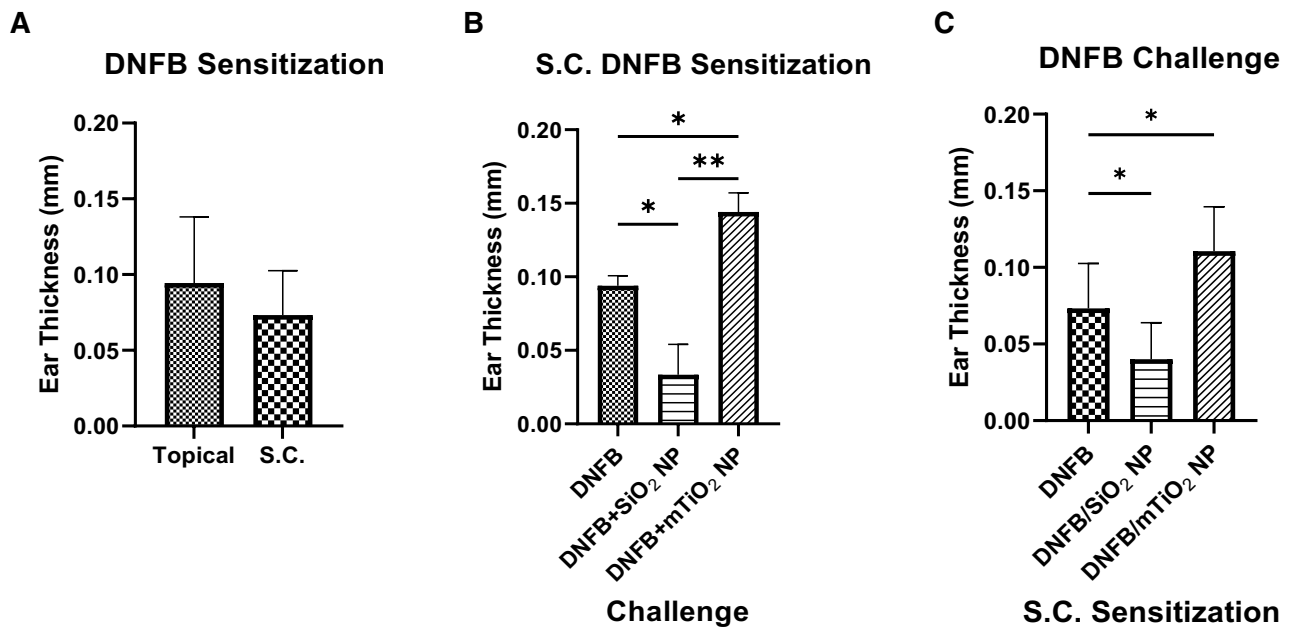


Figure 8. Comparison of CHS allergic response for different models of sensitization and challenge. (A) Comparison of ear swelling response for DNFB topical (0.05%) vs. S.C. (0.01 mM DNFB) sensitization with 0.2% DNFB challenge on one ear vs. vehicle on the other. No differences between these sensitization methods was observed. (B) Comparison of ear swelling response for S.C. sensitization with DNFB only and challenge with DNFB or DNFB co-exposure with NPs and vehicle on the other. Ear swelling was exacerbated with mTiO₂ NPs but decreased with SiO₂ NPs compared to DNFB alone. Ordinary one-way ANOVA was performed and compared to imDC (*). N = 3–12. Mean ± SD. *p < 0.05, **p < 0.01. (C) Comparison of ear swelling response for S.C. sensitization with BMDC treated 1 h with DNFB only or DNFB + SiO₂ or DNFB + mTiO₂ and challenge with 0.2% DNFB on one ear vs. vehicle on the other. Ear swelling was exacerbated with mTiO₂ but decreased with SiO₂ compared to DNFB alone.

increase in ear swelling relative to DNFB alone (Fig. 8C). These results suggest that BMDCs co-cultured with NPs and a potent sensitizer can alter the BMDC phenotype to effect the efficiency of T cell priming and the intensity of the CHS response. In prior work we did not measure an effect of NPs co-exposed topically with DNFB in the sensitization phase²¹. This is most likely due to the inability of the NPs to breach the skin barrier to an appreciable extent to interact sufficiently with skin dendritic cells to alter their phenotype.

Discussion

Engineered NPs have broad applications in many industries and are extensively under development for biomedical use^{62–64}. For example, NPs are being engineered for use in vaccine development where they act as adjuvants and/or carriers to generate antigen-specific tolerogenic adaptive immunity⁶⁴. This is a superior therapeutic strategy compared to suppressing the entire immune system which, can cause long-term damage⁶⁵. Hence, at the forefront of the nanomedicine and nanotoxicology fields, is the need to understand and control how NPs interact with the immune system⁶⁶.

This work expands on our previous studies that showed NPs can modulate the adaptive immune response in a CHS mouse model²¹. We showed that SiO₂ NPs suppressed the allergic response in the challenge phase and mTiO₂ NPs exacerbated it^{21–23}. The mechanism of how these NPs can alter adaptive immune responses remains unclear, which motivated this investigation to examine how these NPs could impact dendritic cell phenotype and function by quantifying BMDC cytotoxicity, cytokine production, the expression of the B7 family co-stimulatory ligands, and the *in vivo* adoptive transfer CHS model.

Results of this study show that BMDC treated with DNFB or mTiO₂, as a function of time and increasing concentration, are cytotoxic (Fig. 1) and they produce higher levels of proinflammatory cytokines (Fig. 2) compared to SiO₂ which exhibited a cytoprotective effect in DNFB co-culture studies whereas mTiO₂ exacerbated DNFB cytotoxicity (Fig. 5). TEM studies confirm that both NPs were taken up by the BMDCs and it showed that DNFB exposure caused BMDCs to lose dendrites and increase the presence of lysosomes (Fig. S2), which degrade exogenous materials⁶⁷. mTiO₂ exposure induced a significant presence of lipid droplets whereas SiO₂ exposure showed only a small increase (Fig. S2). An increase in lipid droplets may result from oxidative stress⁶⁸, or it may indicate upregulation in metabolic activity through glycolysis which also drives the secretion of inflammatory cytokines⁶⁹.

Analysis of the B7 family of co-stimulatory ligands suggest that DNFB and mTiO₂ induce a proinflammatory BMDC (CD11c, MHCII+) phenotype by up-regulating CD86, CD80 and PD-L1 (Fig. 3) similar to LPS (Fig. S10) whereas, SiO₂ had little effect and in fact promoted a more naïve phenotype by inducing a decrease in the percent of CD86 + CD80+ cells over time (Fig. 4). Dendritic cells expressing low levels of CD80/CD86 present antigen

poorly and may induce tolerance^{47,48}. We observed that potent proinflammatory stressors (LPS, DNFB, mTiO₂) upregulate the immunosuppressive PD-L1 ligand (Fig. 3, Fig. S12) which, is a mechanism by which the PD-1/PD-L1 pathway balances the pro-inflammatory effect by promoting the development of Foxp3+ Tregs to limit the immune responses^{43,45,70,71}.

The co-stimulatory molecule CD276 was found to be prominently expressed only on CD80+ cells (Fig. 4, Fig. S13) which, binds the inhibitory CTLA-4 receptor with high affinity^{49,50}. Despite its link to promoting an immunosuppressive BMDC phenotype following activation of the arylhydrocarbon receptor⁶⁰, CD276 expression was down regulated by both NPs in our DNFB co-culture studies (Fig. 6), suggesting that CD276 plays a minimal role driving the adaptive immune response in this CHS adoptive transfer model. Both NPs induced similar effects in modulating the expression levels of CD86, CD80, PD-L1 and CD276 induced by DNFB with the key exception of PD-L2, where mTiO₂ downregulated PD-L2 on the activated CD86+ CD80+ subpopulation and SiO₂ did not (Figs. 6 and 7). This suggests an important role of PD-L2 in directing the efficiency T cell priming in the DNFB-CHS model where SiO₂ treated BMDC suppresses the allergic response in both the sensitization and challenge phases whereas, mTiO₂ exacerbated it (Fig. 8). This finding is consistent with studies of allergic asthma, that showed PD-L2 expression in the lung was protective against the initiation and progression of airway inflammation^{72–75}. Our results point to the importance of PD-L2 expression in the sensitization phase with DNFB, a T_H1 skewing hapten^{76,77}. Studies suggest that PD-L1 and PD-L2 participate in the differential regulation of T_H1 and T_H2 cells⁷⁸. The PD-L1/PD-1 interaction causes a T_H2 response and an increased IL-4 secretion while the PD-L2/PD-1 interaction causes a T_H1 response and an increase in INF- γ secretion⁷³. In future studies it would be important to analyze full cytokine panels that contain T cell polarizing signals as well as chemokines important for lymph node trafficking. Quantifying the expression of the chemokine receptor CCR7 on the engineered BMDC is important as upregulation directs their migration to T-cell zones in lymph nodes⁷⁹. The percent of the S.C. injected BMDC that traffic to the lymph node could be determined using fluorescently labeled BMDC and correlated to CCR7 expression. Quantifying these metrics is important for engineering tolerogenic dendritic cell therapies for treating autoimmune and severe allergic disorders^{65,80}.

While our studies point to differences in PD-L2 expression as a potential mechanism for the differential effects of SiO₂ and mTiO₂ on DNFB sensitization (Fig. 8), it is important to note that the adoptive transfer of ex vivo engineered BMDC preparations contains a heterogeneous mix of B7 phenotypes. Additional studies would be informative to examine the relative importance of each BMDC subset more fully in driving the allergic response. Specifically, the different CD86/CD80 subpopulations (DP, DN, single positive) could be sorted to test which phenotype induces potent allergic responses. Studies show that dendritic cells expressing high levels of CD80 but not CD86 are protective and can induce immune tolerance via promoting CD25+ regulatory T cells⁸¹. It is also important to investigate the effect of protein coronas that form on NPs exposed to biological fluids and cell culture media^{82,83}. Differences in the corona protein composition or abundance could alter the NPs interaction with the BMDCs. Corona composition is highly dependent on surface charge⁸⁴. SiO₂ and mTiO₂ are both negatively charged so we anticipate that similar compositional coronas would form but this should be confirmed in proteomics studies. It is also possible that culturing BMDC with DNFB may haptenize the cells making them directly antigenic. Injection of haptenized BMDC could activate endogenous antigen presenting cells (APCs) in the skin or in the lymph node. Sensitization via this mechanism could be confirmed using transgenic mouse models with deleted endogenous APCs, however, the striking differential effects of the NPs observed in sensitization phase suggest a role for the ex vivo engineered BMDC in directing the observed adaptive immune responses.

This study corroborated our earlier studies using topical DNFB sensitization that showed (Fig. 8B) these NPs affected the allergic response in the challenge phase with mTiO₂ exacerbating the ear swelling and SiO₂ suppressing it²¹. While the mechanism in the challenge phase remains unclear, it seems plausible that the NPs could modulate epidermal-derived signals that affect MC and/or DC activation. These signals could be alarmins produced by keratinocytes or the NPs could modulate of the endogenous expression of CD80 or CD86 on keratinocytes. Studies using transgenic mouse models that over expressed CD80 or CD86 on basal keratinocytes showed a differential ability induce a chronic inflammatory response in the DNFB CHS model⁸⁵. The immunomodulation IL-10 cytokine was also persistently increased in the mouse ear skin in the CD80 transgenic mouse which is consistent with a potent proinflammatory response observed with LPS and mTiO₂ treatment in this study.

In summary, this work points to metrics that can be used to predict the effects of NPs on contact allergy and points to the novel use of NPs to engineer immunomodulatory responses in contact allergy. Given that skin contact allergy is on the rise^{1,2}, as is the creation of novel engineered nanomaterials for industrial, biomedical and consumer use^{62–64,86}, there is a need for assays that can predict the impact that NPs may have on the immune response in the context of skin allergic disease. Further, immunoengineering is an important growing field for developing cell-based therapies to induce antigen specific immune tolerance^{42,64,87,88}.

Materials and methods

Animals

Hairless SKH mice back-crossed 6 generations with C57BL/6 mice were used in this study and all previous work^{21–24}. All animal experimental protocols were reviewed and approved by the University of Rochester Committee on Animal Resources (UCAR #2010-24E). Experiments involving animals and reporting of data were carried out in compliance with the ARRIVE guidelines and all methods were carried out in accordance with relevant guidelines and regulations.

Cell culture

BMDCs were harvested and cultured from tibiae and femurs of 8–12 weeks mice using a standard protocols⁸⁹. Bone marrow cells were suspended in: RPMI 1640 (Gibco Cat# 11875-093) containing 10% FBS (Gibco Cat#

10082147), 1% pen strep (Gibco Cat# 15140-122), 2 mM Glutamax (Gibco Cat# 35050-061), 1 mM sodium pyruvate (Gibco Cat# 11360-070), 50 μ M β -ME (Gibco Cat# 31350-010), and 20 ng/mL GM-CSF (Gibco Cat# PMC2011). A flow cytometry panel was defined (Table S1) to characterize the development of BMDCs over time. While GM-CSF-derived BMDC cultures are heterogeneous, studies confirm they are comprised conventional DCs⁹⁰ and BMDCs are extensively used in both fundamental research and in clinical protocols⁹¹. After 8 days of culture the majority of cells were CD11c+ (86.1%), CD11b+ (98.1%) and MHCII+ (67.6%) with no detection of T or B cells (Fig. S16). On average 10% of cells stain positive for F4/80 a macrophage marker and 71.3% of the cells were CD11c+, CD11b+ and MHCII+ triple positive. Eight-day old BMDCs were used for initiating all experiments.

SiO₂ and mTiO₂ NP characterization

Using dynamic light scattering and zeta potential measurements the SiO₂ NPs (nanoComposix Cat# SISN20-25M) exhibited a hydrodynamic diameter of 33.5 nm (\pm 3.3 nm), zeta potential of -21.9 mV (\pm 10.1 mV) and a PDI of 0.236 in ultrapure water (pH 6.5)²³. The mTiO₂ NPs (Sigma-Aldrich Cat# 677469, < 100 nm) exhibited a hydrodynamic diameter of 556.4 nm (\pm 34.4 nm), zeta potential of -9.05 mV (\pm 1.3 mV) and a PDI of 0.296 in ultrapure water (pH 6.5)²². The lower surface charge on the mTiO₂ NPs suggest a greater tendency to agglomerate as is evidenced by the hydrodynamic diameter being larger than the vendor reported primary size particle size < 100 nm. Transmission electron microscope (TEM, Hitachi 7650) was also used to measure free NPs and NPs inside the cells. The average size of the NPs inside the cells, which for mTiO₂ NPs was found to be 51.6 ± 12.5 nm and SiO₂ NPs were found to be 20.6 ± 3.5 nm (Figs. S3, S4).

Generation of BMDCs exposed to DNFB, SiO₂, and mTiO₂ NPs

The BMDCs were exposed to DNFB, SiO₂, or mTiO₂ at different concentrations for 1 h and non-cytotoxic concentrations (0.001 mM DNFB, 0.01 mg/mL Si20 nm and 0.005 mg/mL mTiO₂) were chosen for the 24 h time studies and subsequent single exposure experiments. The co-exposure of DNFB with SiO₂ NPs did not give any discernible toxicity in vitro, for which, the concentration of DNFB was increased ten-fold (0.01 mM) for some experiments. The concentrations for the co-exposure of DNFB with mTiO₂ NPs remained at 0.001 mM and 0.005 mg/mL, respectively.

Flow cytometry

For cell staining and analysis of co-stimulatory molecule expression, the antibodies and the concentrations used per 1 M cells are summarized in Table S1. We used flow cytometry (Cytek Aurora, Cytek Biosciences) and FlowJo (v10.7.2) to analyze cells. The gating strategy is shown in Fig. S10A. For each experiment FMO controls with BMDC are used. Examples of the FMO gating are illustrated in Fig. S10B,C.

Cytotoxicity and cytokine analysis

Cytotoxicity was measured by flow cytometry using the eFluor™ 780 viability dye that labels dead cells. We normalized the BMDCs live population against imDC control cells that were not treated with any stressor. In addition, we used the PrestoBlue cytotoxicity assay (Invitrogen, P50200) according to manufacture protocol, to confirm the trends observed using flow cytometry. The cell culture supernatant was collected and analyzed for the pro-inflammatory cytokines IL-6, TNF α and the immunosuppressive cytokine IL-10 by ELISA (Invitrogen Cat# 88-7064, 88-7324 and 88-7105, respectively) following manufacture instructions. These cytokines were selected as they represent important innate proinflammatory and immunosuppressive makers.

Contact hypersensitivity (CHS) mouse model

As in our prior work²¹, mice were sensitized topically on the back by applying 20 μ L DNFB (0.05%) diluted in an acetone and olive oil vehicle in a 4:1 ratio. After 5 days, we performed challenge with 20 μ L of 0.2% DNFB on one ear and vehicle (4:1 acetone and olive oil ratio) on the other ear. Alternatively, we sensitized the mice subcutaneously (S.C) by injecting BMDCs (2×10^6) treated for 1 h with DNFB (0.01 mM) only or DNFB (0.01 mM) plus NPs; SiO₂ (0.01 mg/mL) or mTiO₂ (0.005 mg/mL). After 5 days, we performed challenge with 20 μ L of 0.2% DNFB on one ear, and the other ear treated with vehicle (4:1 acetone and olive oil ratio) or 0.2% DNFB plus SiO₂ or mTiO₂ NPs using the same doses and protocols in prior work^{22,23}. The magnitude of the allergic response post challenge was quantified by measuring ear thickness using a digital caliper (Mitutoyo Cat# 209-931) with a resolution of 0.005 mm on day 5, before the application of the challenge dose (pre-challenge). On day 6, both ears were remeasured (post-challenge). Ear swelling (mm) was measured as: (post-challenge) – (pre-challenge).

Statistics

We used GraphPad Prism 9 to analyze all statistical analyses. Ordinary one-way or two-way analysis of variance (ANOVA) was used to compare expression levels of co-stimulatory molecules to imDC (*) and DNFB (#). imDC were not treated with any stressor and served as control. Two-tailed, unpaired with unequal variances, student's t-test was used to compare the ear thickness between two different sensitizing treatments in the CHS in vivo study. p-values < 0.05 were considered significant. All data are presented with standard deviation. The experiments were replicated at least three times.

Data availability

All data are available in the main text or the supplementary materials. Raw data will be made available upon request. Contact: Lisa DeLouise: lisa_delouise@urmc.rochester.edu.

Received: 15 June 2023; Accepted: 14 September 2023

Published online: 25 September 2023

References

1. Salah, S., Taieb, C., Demessant, A. L. & Haftek, M. Prevalence of skin reactions and self-reported allergies in 5 countries with their social impact measured through quality of life impairment. *Int. J. Environ. Res. Public Health*. <https://doi.org/10.3390/ijerph18094501> (2021).
2. Owen, J. L., Vakharia, P. P. & Silverberg, J. I. The role and diagnosis of allergic contact dermatitis in patients with atopic dermatitis. *Am. J. Clin. Dermatol.* **19**, 293–302. <https://doi.org/10.1007/s40257-017-0340-7> (2018).
3. Thyssen, J. P., Linneberg, A., Menne, T. & Johansen, J. D. The epidemiology of contact allergy in the general population—prevalence and main findings. *Contact Dermat.* **57**, 287–299. <https://doi.org/10.1111/j.1600-0536.2007.01220.x> (2007).
4. Nosbaum, A., Vocanson, M., Rozieres, A., Hennino, A. & Nicolas, J. F. Allergic and irritant contact dermatitis. *Eur. J. Dermatol.* **19**, 325–332. <https://doi.org/10.1684/ejd.2009.0686> (2009).
5. Roberts, D. W. Allergic contact dermatitis: Is the reactive chemistry of skin sensitizers the whole story? A response. *Contact Dermat.* **68**, 245–249. <https://doi.org/10.1111/cod.12057> (2013).
6. Brys, A. K., Rodriguez-Homs, L. G., Suwanpradit, J., Atwater, A. R. & MacLeod, A. S. Shifting paradigms in allergic contact dermatitis: The role of innate immunity. *J. Investig. Dermatol.* **140**, 21–28. <https://doi.org/10.1016/j.jid.2019.03.1133> (2020).
7. Honda, T., Egawa, G., Grabbe, S. & Kabashima, K. Update of immune events in the murine contact hypersensitivity model: Toward the understanding of allergic contact dermatitis. *J. Investig. Dermatol.* **133**, 303–315. <https://doi.org/10.1038/jid.2012.284> (2013).
8. Gamradt, P. et al. Inhibitory checkpoint receptors control CD8(+) resident memory T cells to prevent skin allergy. *J. Allergy Clin. Immunol.* **143**, 2147–2157 e2149. <https://doi.org/10.1016/j.jaci.2018.11.048> (2019).
9. Ho, A. W. & Kupper, T. S. T cells and the skin: From protective immunity to inflammatory skin disorders. *Nat. Rev. Immunol.* **19**, 490–502. <https://doi.org/10.1038/s41577-019-0162-3> (2019).
10. Kantor, R. & Silverberg, J. I. Environmental risk factors and their role in the management of atopic dermatitis. *Expert Rev. Clin. Immunol.* **13**, 15–26. <https://doi.org/10.1080/1744666X.2016.1212660> (2017).
11. Jenerowicz, D. et al. Environmental factors and allergic diseases. *Ann. Agric. Environ. Med.* **19**, 475–481 (2012).
12. Kim, J. et al. Symptoms of atopic dermatitis are influenced by outdoor air pollution. *J. Allergy Clin. Immunol.* **132**, 495–498 e491. <https://doi.org/10.1016/j.jaci.2013.04.019> (2013).
13. Smita, S. et al. Nanoparticles in the environment: Assessment using the causal diagram approach. *Environ. Health* **11**(Suppl 1), S13. <https://doi.org/10.1186/1476-069X-11-S1-S13> (2012).
14. Drakaki, E., Dessinioti, C. & Antoniou, C. V. Air pollution and the skin. *Front. Environ. Sci.-Switz.* <https://doi.org/10.3389/fenvs.2014.00011> (2014).
15. Kapoor, D. & Singh, M. P. In *Plant Responses to Nanomaterials: Recent Interventions, and Physiological and Biochemical Responses* (eds. Singh, V. P. et al.) 217–232 (Springer International Publishing, 2021).
16. Magnani, N. D. et al. Skin damage mechanisms related to airborne particulate matter exposure. *Toxicol. Sci.* **149**, 227–236. <https://doi.org/10.1093/toxsci/kfv230> (2016).
17. Seet, R. C. et al. Biomarkers of oxidative damage in cigarette smokers: Which biomarkers might reflect acute versus chronic oxidative stress?. *Free Radic. Biol. Med.* **50**, 1787–1793. <https://doi.org/10.1016/j.freeradbiomed.2011.03.019> (2011).
18. Sahu, R. P. et al. Cigarette smoke exposure inhibits contact hypersensitivity via the generation of platelet-activating factor agonists. *J. Immunol.* **190**, 2447–2454. <https://doi.org/10.4049/jimmunol.1202699> (2013).
19. Ocana, J. A. et al. Platelet-activating factor-induced reduction in contact hypersensitivity responses is mediated by mast cells via cyclooxygenase-2-dependent mechanisms. *J. Immunol.* **200**, 4004–4011. <https://doi.org/10.4049/jimmunol.1701145> (2018).
20. Jatana, S., Palmer, B. C., Phelan, S. J., Gelein, R. & DeLouise, L. A. In vivo quantification of quantum dot systemic transport in C57BL/6 hairless mice following skin application post-ultraviolet radiation. *Part Fibre Toxicol.* **14**, 12. <https://doi.org/10.1186/s12989-017-0191-7> (2017).
21. Jatana, S., Palmer, B. C., Phelan, S. J. & DeLouise, L. A. Immunomodulatory effects of nanoparticles on skin allergy. *Sci. Rep.* **7**, 3979. <https://doi.org/10.1038/s41598-017-03729-2> (2017).
22. Palmer, B. C. & DeLouise, L. A. Morphology-dependent titanium dioxide nanoparticle-induced keratinocyte toxicity and exacerbation of allergic contact dermatitis. *HSOA J. Toxicol.* <https://doi.org/10.24966/tcr-3735/100019> (2020).
23. Palmer, B. C., Jatana, S., Phelan-Dickinson, S. J. & DeLouise, L. A. Amorphous silicon dioxide nanoparticles modulate immune responses in a model of allergic contact dermatitis. *Sci. Rep.* **9**, 5085. <https://doi.org/10.1038/s41598-019-41493-7> (2019).
24. Palmer, B. C., Phelan-Dickinson, S. J. & DeLouise, L. A. Multi-walled carbon nanotube oxidation dependent keratinocyte cytotoxicity and skin inflammation. *Part Fibre Toxicol.* **16**, 3. <https://doi.org/10.1186/s12989-018-0285-x> (2019).
25. Jatana, S., Callahan, L. M., Pentland, A. P. & DeLouise, L. A. Impact of cosmetic lotions on nanoparticle penetration through ex vivo C57BL/6 hairless mouse and human skin: A comparison study. *Cosmetics* <https://doi.org/10.3390/cosmetics3010006> (2016).
26. Mortensen, L. J., Oberdorster, G., Pentland, A. P. & DeLouise, L. A. In vivo skin penetration of quantum dot nanoparticles in the murine model: The effect of UVR. *Nano Lett.* **8**, 2779–2787. <https://doi.org/10.1021/nl801332y> (2008).
27. Liang, X. W. et al. Penetration of nanoparticles into human skin. *Curr. Pharm. Des.* **19**, 6353–6366. <https://doi.org/10.2174/1381612811319350011> (2013).
28. Schneider, M., Stracke, F., Hansen, S. & Schaefer, U. F. Nanoparticles and their interactions with the dermal barrier. *Dermatoendocrinology* **1**, 197–206. <https://doi.org/10.4161/derm.1.4.9501> (2009).
29. Roberts, D. W., Mekenyan, O. G., Dimitrov, S. D. & Dimitrova, G. D. What determines skin sensitization potency—myths, maybes and realities. Part 1. The 500 molecular weight cut-off. *Contact Dermat.* **68**, 32–41. <https://doi.org/10.1111/j.1600-0536.2012.02160.x> (2013).
30. Carroll-Portillo, A. et al. Mast cells and dendritic cells form synapses that facilitate antigen transfer for T cell activation. *J. Cell Biol.* **210**, 851–864. <https://doi.org/10.1083/jcb.201412074> (2015).
31. Sumpster, T. L., Balmert, S. C. & Kaplan, D. H. Cutaneous immune responses mediated by dendritic cells and mast cells. *JCI Insight* <https://doi.org/10.1172/jci.insight.123947> (2019).
32. Otsuka, A. et al. Requirement of interaction between mast cells and skin dendritic cells to establish contact hypersensitivity. *PLoS ONE* **6**, e25538. <https://doi.org/10.1371/journal.pone.0025538> (2011).
33. Dudeck, A. et al. Mast cells are key promoters of contact allergy that mediate the adjuvant effects of haptens. *Immunity* **34**, 973–984. <https://doi.org/10.1016/j.immuni.2011.03.028> (2011).
34. Suto, H. et al. Mast cell-associated TNF promotes dendritic cell migration. *J. Immunol.* **176**, 4102–4112. <https://doi.org/10.4049/jimmunol.176.7.4102> (2006).
35. Tordesillas, L. et al. PDL2(+) CD11b(+) dermal dendritic cells capture topical antigen through hair follicles to prime LAP(+) Tregs. *Nat. Commun.* **9**, 5238. <https://doi.org/10.1038/s41467-018-07716-7> (2018).
36. Bennett, C. L. et al. Inducible ablation of mouse Langerhans cells diminishes but fails to abrogate contact hypersensitivity. *J. Cell Biol.* **169**, 569–576. <https://doi.org/10.1083/jcb.200501071> (2005).
37. Bursch, L. S. et al. Identification of a novel population of Langerin+ dendritic cells. *J. Exp. Med.* **204**, 3147–3156. <https://doi.org/10.1084/jem.20071966> (2007).

38. Clausen, B. E. & Stoitzner, P. Functional specialization of skin dendritic cell subsets in regulating T cell responses. *Front. Immunol.* **6**, 534. <https://doi.org/10.3389/fimmu.2015.00534> (2015).
39. Poulin, L. F. *et al.* The dermis contains langerin+ dendritic cells that develop and function independently of epidermal Langerhans cells. *J. Exp. Med.* **204**, 3119–3131. <https://doi.org/10.1084/jem.20071724> (2007).
40. Fukunaga, A., Khaskhely, N. M., Sreevidya, C. S., Byrne, S. N. & Ullrich, S. E. Dermal dendritic cells, and not Langerhans cells, play an essential role in inducing an immune response. *J. Immunol.* **180**, 3057–3064. <https://doi.org/10.4049/jimmunol.180.5.3057> (2008).
41. Noordegraaf, M., Flacher, V., Stoitzner, P. & Clausen, B. E. Functional redundancy of Langerhans cells and Langerin+ dermal dendritic cells in contact hypersensitivity. *J. Investig. Dermatol.* **130**, 2752–2759. <https://doi.org/10.1038/jid.2010.223> (2010).
42. Jia, J. *et al.* Interactions between nanoparticles and dendritic cells: From the perspective of cancer immunotherapy. *Front. Oncol.* **8**, 404. <https://doi.org/10.3389/fonc.2018.00404> (2018).
43. Greenwald, R. J., Freeman, G. J. & Sharpe, A. H. The B7 family revisited. *Annu. Rev. Immunol.* **23**, 515–548. <https://doi.org/10.1146/annurev.immunol.23.021704.115611> (2005).
44. Sansom, D. M. CD28, CTLA-4 and their ligands: Who does what and to whom?. *Immunology* **101**, 169–177. <https://doi.org/10.1046/j.1365-2567.2000.00121.x> (2000).
45. Halliday, N. *et al.* CD86 is a selective CD28 ligand supporting FoxP3+ regulatory T cell homeostasis in the presence of high levels of CTLA-4. *Front. Immunol.* **11**, 600000. <https://doi.org/10.3389/fimmu.2020.600000> (2020).
46. Kennedy, A. *et al.* Differences in CD80 and CD86 transendocytosis reveal CD86 as a key target for CTLA-4 immune regulation. *Nat. Immunol.* **23**, 1365–1378. <https://doi.org/10.1038/s41590-022-01289-w> (2022).
47. Lu, P., Wang, Y. L. & Linsley, P. S. Regulation of self-tolerance by CD80/CD86 interactions. *Curr. Opin. Immunol.* **9**, 858–862. [https://doi.org/10.1016/s0952-7915\(97\)80190-2](https://doi.org/10.1016/s0952-7915(97)80190-2) (1997).
48. Saito, K., Yagita, H., Hashimoto, H., Okumura, K. & Azuma, M. Effect of CD80 and CD86 blockade and anti-interleukin-12 treatment on mouse acute graft-versus-host disease. *Eur. J. Immunol.* **26**, 3098–3106. <https://doi.org/10.1002/eji.1830261241> (1996).
49. Hathcock, K. S., Laszlo, G., Pucillo, C., Linsley, P. & Hodes, R. J. Comparative analysis of B7-1 and B7-2 costimulatory ligands: Expression and function. *J. Exp. Med.* **180**, 631–640. <https://doi.org/10.1084/jem.180.2.631> (1994).
50. Thiel, M. *et al.* Efficiency of T-cell costimulation by CD80 and CD86 cross-linking correlates with calcium entry. *Immunology* **129**, 28–40. <https://doi.org/10.1111/j.1365-2567.2009.03155.x> (2010).
51. van der Merwe, P. A., Bodian, D. L., Daenke, S., Linsley, P. & Davis, S. J. CD80 (B7-1) binds both CD28 and CTLA-4 with a low affinity and very fast kinetics. *J. Exp. Med.* **185**, 393–403. <https://doi.org/10.1084/jem.185.3.393> (1997).
52. Granier, C. *et al.* Mechanisms of action and rationale for the use of checkpoint inhibitors in cancer. *ESMO Open* **2**, e000213. <https://doi.org/10.1136/esmoopen-2017-000213> (2017).
53. Yokosuka, T. *et al.* Programmed cell death 1 forms negative costimulatory microclusters that directly inhibit T cell receptor signaling by recruiting phosphatase SHP2. *J. Exp. Med.* **209**, 1201–1217. <https://doi.org/10.1084/jem.20112741> (2012).
54. Philips, E. A. *et al.* The structural features that distinguish PD-L2 from PD-L1 emerged in placental mammals. *J. Biol. Chem.* **295**, 4372–4380. <https://doi.org/10.1074/jbc.AC119.011747> (2020).
55. Solinas, C. *et al.* Programmed cell death-ligand 2: A neglected but important target in the immune response to cancer?. *Transl. Oncol.* **13**, 100811. <https://doi.org/10.1016/j.tranon.2020.100811> (2020).
56. Ghiotto, M. *et al.* PD-L1 and PD-L2 differ in their molecular mechanisms of interaction with PD-1. *Int. Immunol.* **22**, 651–660. <https://doi.org/10.1093/intimm/dxq049> (2010).
57. Loke, P. & Allison, J. P. PD-L1 and PD-L2 are differentially regulated by Th1 and Th2 cells. *Proc. Natl. Acad. Sci. U. S. A.* **100**, 5336–5341. <https://doi.org/10.1073/pnas.0931259100> (2003).
58. Hurrell, B. P. *et al.* PD-L2 controls peripherally induced regulatory T cells by maintaining metabolic activity and Foxp3 stability. *Nat. Commun.* **13**, 5118. <https://doi.org/10.1038/s41467-022-32899-5> (2022).
59. Durlanik, S. *et al.* CD276 is an important player in macrophage recruitment into the tumor and an upstream regulator for PAI-1. *Sci. Rep.* **11**, 14849. <https://doi.org/10.1038/s41598-021-94360-9> (2021).
60. Bruhs, A. *et al.* Activation of the arylhydrocarbon receptor causes immunosuppression primarily by modulating dendritic cells. *J. Investig. Dermatol.* **135**, 435–444. <https://doi.org/10.1038/jid.2014.419> (2015).
61. Mytych, J., Wnuk, M. & Rattan, S. I. Low doses of nanodiamonds and silica nanoparticles have beneficial hormetic effects in normal human skin fibroblasts in culture. *Chemosphere* **148**, 307–315. <https://doi.org/10.1016/j.chemosphere.2016.01.045> (2016).
62. Kessler, R. Engineered nanoparticles in consumer products: Understanding a new ingredient. *Environ. Health Perspect.* **119**, a120–125. <https://doi.org/10.1289/ehp.119-a120> (2011).
63. Khan, L., Saeed, K. & Khan, I. Nanoparticles: Properties, applications and toxicities. *Arab. J. Chem.* **12**, 908–931. <https://doi.org/10.1016/j.arabjc.2017.05.011> (2019).
64. Toy, R. & Roy, K. Engineering nanoparticles to overcome barriers to immunotherapy. *Bioeng. Transl. Med.* **1**, 47–62. <https://doi.org/10.1002/btm2.10005> (2016).
65. Boks, M. A. *et al.* IL-10-generated tolerogenic dendritic cells are optimal for functional regulatory T cell induction—A comparative study of human clinical-applicable DC. *Clin. Immunol.* **142**, 332–342. <https://doi.org/10.1016/j.clim.2011.11.011> (2012).
66. Liu, Y., Hardie, J., Zhang, X. & Rotello, V. M. Effects of engineered nanoparticles on the innate immune system. *Semin. Immunol.* **34**, 25–32. <https://doi.org/10.1016/j.smim.2017.09.011> (2017).
67. Rathore, B. *et al.* Nanomaterial designing strategies related to cell lysosome and their biomedical applications: A review. *Biomaterials* **211**, 25–47. <https://doi.org/10.1016/j.biomaterials.2019.05.002> (2019).
68. Jarc, E. & Petan, T. Lipid droplets and the management of cellular stress. *Yale J. Biol. Med.* **92**, 435–452 (2019).
69. Adeva-Andany, M. M., Gonzalez-Lucan, M., Donapetry-Garcia, C., Fernandez-Fernandez, C. & Ameneiros-Rodriguez, E. Glycogen metabolism in humans. *BBA Clin.* **5**, 85–100. <https://doi.org/10.1016/j.bbaci.2016.02.001> (2016).
70. Neumann, K. *et al.* The co-inhibitory molecule PD-L1 contributes to regulatory T cell-mediated protection in murine crescentic glomerulonephritis. *Sci. Rep.* **9**, 2038. <https://doi.org/10.1038/s41598-018-38432-3> (2019).
71. Yamaguchi, H., Hsu, J. M., Yang, W. H. & Hung, M. C. Mechanisms regulating PD-L1 expression in cancers and associated opportunities for novel small-molecule therapeutics. *Nat. Rev. Clin. Oncol.* **19**, 287–305. <https://doi.org/10.1038/s41571-022-00601-9> (2022).
72. Akbari, O. *et al.* PD-L1 and PD-L2 modulate airway inflammation and iNKT-cell-dependent airway hyperreactivity in opposing directions. *Mucosal Immunol.* **3**, 81–91. <https://doi.org/10.1038/mi.2009.112> (2010).
73. Singh, A. K., Stock, P. & Akbari, O. Role of PD-L1 and PD-L2 in allergic diseases and asthma. *Allergy* **66**, 155–162. <https://doi.org/10.1111/j.1398-9995.2010.02458.x> (2011).
74. Matsumoto, K. *et al.* B7-DC induced by IL-13 works as a feedback regulator in the effector phase of allergic asthma. *Biochem. Biophys. Res. Commun.* **365**, 170–175. <https://doi.org/10.1016/j.bbrc.2007.10.156> (2008).
75. Matsumoto, K. *et al.* B7-DC regulates asthmatic response by an IFN-gamma-dependent mechanism. *J. Immunol.* **172**, 2530–2541. <https://doi.org/10.4049/jimmunol.172.4.2530> (2004).
76. Dearman, R. J., Basketter, D. A. & Kimber, I. Characterization of chemical allergens as a function of divergent cytokine secretion profiles induced in mice. *Toxicol. Appl. Pharmacol.* **138**, 308–316. <https://doi.org/10.1006/taap.1996.0129> (1996).

77. Hayashi, M., Higashi, K., Kato, H. & Kaneko, H. Assessment of preferential Th1 or Th2 induction by low-molecular-weight compounds using a reverse transcription-polymerase chain reaction method: Comparison of two mouse strains, C57BL/6 and BALB/c. *Toxicol. Appl. Pharmacol.* **177**, 38–45. <https://doi.org/10.1006/taap.2001.9286> (2001).
78. Xiao, Y. *et al.* RGMb is a novel binding partner for PD-L2 and its engagement with PD-L2 promotes respiratory tolerance. *J. Exp. Med.* **211**, 943–959. <https://doi.org/10.1084/jem.20130790> (2014).
79. Riol-Blanco, L. *et al.* The chemokine receptor CCR7 activates in dendritic cells two signaling modules that independently regulate chemotaxis and migratory speed. *J. Immunol.* **174**, 4070–4080. <https://doi.org/10.4049/jimmunol.174.7.4070> (2005).
80. Moorman, C. D., Sohn, S. J. & Phee, H. Emerging therapeutics for immune tolerance: Tolerogenic vaccines, T cell therapy, and il-2 therapy. *Front. Immunol.* **12**, 657768. <https://doi.org/10.3389/fimmu.2021.657768> (2021).
81. Ke, N., Su, A., Huang, W., Szatmary, P. & Zhang, Z. Regulating the expression of CD80/CD86 on dendritic cells to induce immune tolerance after xeno-islet transplantation. *Immunobiology* **221**, 803–812. <https://doi.org/10.1016/j.imbio.2016.02.002> (2016).
82. Docter, D. *et al.* The nanoparticle biomolecule corona: Lessons learned—challenge accepted?. *Chem. Soc. Rev.* **44**, 6094–6121. <https://doi.org/10.1039/c5cs00217f> (2015).
83. Kim, W. *et al.* Protein corona: Friend or foe? Co-opting serum proteins for nanoparticle delivery. *Adv. Drug Deliv. Rev.* **192**, 114635. <https://doi.org/10.1016/j.addr.2022.114635> (2023).
84. Xiao, B., Liu, Y., Chandrasiri, I., Overby, C. & Benoit, D. S. W. Impact of nanoparticle physicochemical properties on protein corona and macrophage polarization. *ACS Appl. Mater. Interfaces* <https://doi.org/10.1021/acsmi.2c22471> (2023).
85. Burns, R. *et al.* Keratinocyte-derived, CD80-mediated costimulation is associated with hapten-specific IgE production during contact hypersensitivity to TH1 haptens. *J. Allergy Clin. Immunol.* **115**, 383–390. <https://doi.org/10.1016/j.jaci.2004.11.019> (2005).
86. Salata, O. Applications of nanoparticles in biology and medicine. *J. Nanobiotechnol.* **2**, 3. <https://doi.org/10.1186/1477-3155-2-3> (2004).
87. Kishimoto, T. K. & Maldonado, R. A. Nanoparticles for the induction of antigen-specific immunological tolerance. *Front. Immunol.* **9**, 230. <https://doi.org/10.3389/fimmu.2018.00230> (2018).
88. LaMothe, R. A. *et al.* Tolerogenic nanoparticles induce antigen-specific regulatory T cells and provide therapeutic efficacy and transferrable tolerance against experimental autoimmune encephalomyelitis. *Front. Immunol.* **9**, 281. <https://doi.org/10.3389/fimmu.2018.00281> (2018).
89. Sauter, M. *et al.* Protocol to isolate and analyze mouse bone marrow derived dendritic cells (BMDC). *STAR Protoc.* **3**, 101664. <https://doi.org/10.1016/j.xpro.2022.101664> (2022).
90. Helft, J. *et al.* GM-CSF mouse bone marrow cultures comprise a heterogeneous population of CD11c(+)MHCII(+) macrophages and dendritic cells. *Immunity* **42**, 1197–1211. <https://doi.org/10.1016/j.immuni.2015.05.018> (2015).
91. Abdi, K. *et al.* Bone marrow-derived dendritic cell cultures from RAG(−/−) mice include IFN- γ -producing NK cells. *Immunohorizons* **4**, 415–419. <https://doi.org/10.4049/immunohorizons.2000011> (2020).

Acknowledgements

This work was supported by a grant from the National Institute of Environmental Health Sciences, R01ES021492.

Author contributions

L.A.D. contributed to the conceptualization of the work. J.P.P. helped generate the CHS mouse data. A.W.L. generated all of the flow data, figures and statistical analysis. L.A.D., A.W.L. contributed to the study design, discussion of the results, and writing of the manuscript.

Competing interests

The authors declare no competing interests.

Additional information

Supplementary Information The online version contains supplementary material available at <https://doi.org/10.1038/s41598-023-42797-5>.

Correspondence and requests for materials should be addressed to L.A.D.

Reprints and permissions information is available at www.nature.com/reprints.

Publisher's note Springer Nature remains neutral with regard to jurisdictional claims in published maps and institutional affiliations.



Open Access This article is licensed under a Creative Commons Attribution 4.0 International License, which permits use, sharing, adaptation, distribution and reproduction in any medium or format, as long as you give appropriate credit to the original author(s) and the source, provide a link to the Creative Commons licence, and indicate if changes were made. The images or other third party material in this article are included in the article's Creative Commons licence, unless indicated otherwise in a credit line to the material. If material is not included in the article's Creative Commons licence and your intended use is not permitted by statutory regulation or exceeds the permitted use, you will need to obtain permission directly from the copyright holder. To view a copy of this licence, visit <http://creativecommons.org/licenses/by/4.0/>.

© The Author(s) 2023